International Journal of Environmental Sciences
ISSN: 2229-7359
Vol. 11 No. 8s, 2025
https://www.theaspd.com/ijes.php

A Review On Metal Oxide Nano-Materials For Water Treatment

Kavya M P M[1], Dr. P. Shiva Keshava Kumar[2]
[1]Department of Civil Engineering, Rajarajeswari College of Engineering, Bengaluru, Karnataka, India,
Email: kavyavagm@gmail.com
[2]Department of Civil Engineering, Proudadevaraya Institute of Technology, Hospet, Karnataka, India
Email: drshivakeshava@gmail.com
Corresponding Author: Dr. P Shiva Keshava Kumar, drshivakeshava@gmail.com

Abstract
In today's world, nanotechnology is becoming increasingly popular for water treat- ment. In this review paper, we will summarize recent advances in the development of typical metal oxide materials (TiO_2, Fe_3O_4/Fe_2O_3, MnO_2, CeO_2, MgO and Al_2O_3) and the related processes for the treatment of various water resources which have been contaminated by organic solutes, inorganic anions, radionuclides, bacteria and viruses.

Keywords: *Metal oxide nanomaterials; Water treatment; Photocatalysis; Adsorption; Nanostructures.*

1. INTRODUCTION

In today's world, approximately 20% of the population has no access to safe water, 40% suffers the consequences of unacceptable sanitary conditions, and millions of people die every year from diseases transmitted through unsafe water [1]. More- over, the situation will undoubtedly worsen, in both developing and developed countries, as materials ranging from heavy metals and distillates to microorganisms continue to attack water supplies as contaminants, mainly as a result of human activities. Very recently, Shannon *et al.* claimed that during the coming decades, water scarcity and water stress may become watchwords that prompt action ranging from wholesale population migration to war, unless new, rapid, more effective, low-cost and robust procedures to supply clean water are identified [2].

Fortunately, nanotechnology – with its emerging opportunities – can provide powerful solutions for some environmental problems. Due to their unique activity towards recalcitrant contaminants and the flexibility of their applications, many nanomaterials are currently being examined for the treatment of ground water, surface water and drinking water contaminated by toxic metal ions, organic and inorganic solutes and microorganisms. In particular, metal oxide nanomaterials are undergoing development for environmental monitoring, remediation and pollution prevention, in addition to the effective saving of resources. These properties are based on the rich valence states, vast surfaces and varying electronic structures of nanomaterials. Previously, Theron *et al.* prepared an excellent general review on nanotechnology and water treatment, which described a variety of nanomaterials and their applications for water treatment, purification and disinfection [3]. In this chapter, our intention is to highlight the details of current research investigations into typical metal oxide nanomaterials (TiO_2, Fe_3O_4/Fe_2O_3, MnO_2, CeO_2, MgO and Al_2O_3) and their applications in water treatment. Nano Metal Oxides have proven their potential in several biomedical and phtovolaic applications from targeted drug delivery to magnetic hyperthermia applications. For such application, it is necessary that the NPs to be used must be biocompatible. Besides biocompatibility, water dispersibility is also an essential requirement for these NPs to be used in many biomedical applications such as Magnetic Hyperthermia applications. Semiconducting materials can absorb solar energy and utilize this energy for the transition of electrons from the valence band to the conduction band. This transition leads to create an electron hole pair in the semiconductor materials, and this phenomenon is used to generate the electric energy from the solar energy. Many metal oxides such as ZnO, TiO_2 etc. have good semiconducting properties with a wide band gap.

1.1 Titanium Dioxide (TiO2)

Since the initial discovery of photocatalytic water splitting on titanium dioxide (TiO_2) electrodes [4], much attention has been paid to applying TiO_2 as a high- quality photocatalyst for water treatment. This proposal is based not only on the potential of TiO_2 to degrade a wide range of organic and inorganic compounds, but also on its physical and chemical stability, lower cost and resistance to corrosion [5]. The decrease of TiO_2 particle size into nanoscale will result in a measure of selectivity in the photoreactions and the presence of crystal defects, which in turn will allow the electron-hole separation yield to be maximized [6–8]. During the past few years, many TiO_2 nanostructures – such as nanoparticles, nanotubes/ nanorods, nanofilms and nanocomposites – have been synthesized in various ways and used widely in the treatment of water.

1.2 TiO_2 Nanoparticles

Degradation of Organic Pollutants

From laboratory to plant, the commercially available TiO_2 named Degussa P-25 (30 nm) has been widely used in the treatment of contaminated water, and has indeed become a research standard reference [9, 10]. This two-phase composite (anatase and rutile) has been considered to have a synergy effect for photocatalytic reactions [11].

A smaller titanium dioxide was also used for the degradation of certain organic pollutants. For example, TiO_2 with diameters of G to 10 nm were prepared for the photocatalytic degradation of hexahydro-1,3,5-trinitro-1,3,5-triazine (RDX) waste- water under simulated sunlight [12]. The result showed that the RDX degradation percentage of the photocatalytic process was higher than that of Fenton oxidation before 80 min, equivalent after 80 min, and reached 95% or above after 120 min.

During recent years, the synthesis of doped TiO_2 nanoparticles has attracted increasing attention in organic wastewater treatment [13–17]. For example, Liu et al. introduced a low-cost and high-efficiency approach for preparing nitrogen- doped TiO_2 with a lower band-gap energy which can be responsive to visible light [18]. The N-doped TiO_2 showed superior photocatalytic activities in both chemical compound degradation and bactericidal reactions over commercially available Degussa P25 power, under identical solar light exposure.

As well as nonmetal-doped TiO_2 nanoparticles, metal-doped TiO_2 nanoparticles have also been developed for the degradation of organic pollutants. As an example, Fe(III) doped TiO_2 nanoparticles have been prepared to degrade phenol in water under solar light irradiation [19]. Furthermore, Oh et al. studied the effect of additives (Si, Fe) on the photocatalytic activity of titanium dioxide powders prepared by thermal plasma [20]. Similarly, the photocatalytic degradation of 2-chlorophenol (2-CP) in aqueous solution was evaluated using a Co-doped TiO_2 nanoparticulate catalyst [21]. Specifically, rare earth metal Pr-doped TiO_2 showed a high activity for the photocatalytic degradation of phenol [22], the degradation process having been optimized using 1 g l^{-1} Pr-doped TiO_2 with a Pr(III) concentration of 0.072 mol% after 2 h irradiation. As a systemic study, Shah et al. reported that the metalloorganic chemical vapor deposition (MOCVD) method could be used successfully to synthesize pure TiO_2 and Nd_3+-, Pd_2+-, Pt_4+- and Fe_3+-doped TiO_2 nanoparticles [23]. When the effects of different types of dopant on the photocatalytic activity were investigated by the degradation of 2-CPs in UV light, it was suggested that the negative and positive effects could be ascribed to the position of the dopants in the nanoparticles and the difference in their ionic radii with respect to that of Ti_4+. There is no general way to guide and evaluate the TiO_2-doped photocatalytic activity associated with the relationships of the category, quantity and position of dopant, since doping is referred to as a very complex processes.

Catalysis and Adsorption of Inorganic Anions

Arsenic has, for many centuries, been considered as one of the most toxic elemental contaminants. In the presence of sunlight and dissolved oxygen, Pena et al. investigated the effectiveness of nanocrystalline TiO_2 in removing arsenate [As(V)], arsenite [As(III)] and the photocatalytic oxidation of As(III) [24]. These studies revealed that the TiO_2 was effective for arsenic removal at pH 8, and had a maximum removal quantity for As(III) at pH approximately 7.5 in the challenging water. Moreover, the adsorption capacity of the TiO_2 for

As(V) and As(III) was much higher than that of the commercial TiO_2 (Degussa P-25) and granular ferric oxide. Cr(VI) represents another typical (and also carcinogenic) pollutant that is found in the wastewater from industrial processes, such as mining, leather tanning and paint-making. In a typical treatment process, Cr(VI) can be reduced to less toxic Cr(III) by reducing agents, although this usually leads to a much larger dosage of the reducing agent than the stoichiometric amount. To overcome this drawback, photocatalytic reduction – as an environment-friendly treatment process – has been developed and proven effective in the reduction of Cr(VI) to Cr(III). For example, when TiO_2 and sulfated TiO_2-SO_2-TiO_2 catalysts with different textural proper- ties were prepared for the photocatalytic reduction of Cr(VI) to Cr(III) [25], the calcination temperature was shown to be a key factor that affected the catalytic activities. Consequently, the research group involved suggested that SO_2 on the surface could provide an acid environment over the catalyst surface and in turn promote the photoreduction of Cr(VI).

Disinfection of Microorganisms

When titanium dioxide nanoparticles and nanocrystalline are irradiated with UV- visible light, this semiconductor can exhibit strong bactericidal activity. For instance, Chang et al. showed that the irradiation of suspensions of Escherichia coli and TiO_2 (P-25) with of wavelengths longer than 380 nm led to bactericidal action within minutes [26]. Furthermore, the trends in these simulated laboratory experiments were mimicked in outdoor tests conducted under the summer, noonday sun [27]. Elsewhere, Maness et al. presented the first evidence that lipid peroxidation reaction was the underlying mechanism of cell death of E. coli K-12 irradiated in the presence of a TiO_2 photocatalyst [28]. These authors claimed that the TiO_2 photocatalysis initiated peroxidation of the unsaturated phospholipid component of the lipid membrane, thus inducing a major disorder in the E. coli cell membrane and killing the cells. TiO_2 nanoparticles, as-doped, could also be used for the disinfection of waste- water. For example, Yu et al. reported that sulfur-doped titanium dioxide exhibited a strong visible-light-induced antibacterial effect [29], while Egerton et al. found that the photo electrocatalytic disinfection of E. coli by an iron-doped TiO_2 sol–gel electrode was more efficient than disinfection by the corresponding electrode when undoped [30].

1.3 TiO_2 Nanotubes and Nanorods

The band-gap of aqueous colloids of titanate nanotubes at room temperature has been estimated at approximately 3.87 eV, which is close to the value of about 3.84 eV in two-dimensional (2-D) titanate nanosheets, but much higher than the value of about 3.2 eV in bulk TiO_2 [31, 32]. Three general approaches – namely alkaline hydrothermal [33], template-assisted [34] and anodic oxidation [35] – for the preparation of nanostructured titanate and TiO_2 have been reviewed by Bavykin [36]. TiO_2 nanotubes have potential applications in solar cells and hydrogen pro- duction [37–41], although the details of TiO_2 nanotubes, which were developed directly for the photocatalytic removal of organic pollutants, have been rarely reported.

As a typical study, the synthesis of TiO_2-based p-n junction nanotubes has been described [42]. The outside of the tubes was comprised of TiO_2, and the inside platinum. The nature of the p-n junction allowed the outside of the tube to act as an oxidizing surface, while the inside of the tube acted as a reductive surface. When exposed to UV light, these catalysts were able to degrade toluene, with experimental results showing that the photocatalytic destruction rates of these catalysts were higher than those of non-nanotube-structured material and nano- tubes without a p-n junction.

Moreover, titanate nanotubes can adsorb functional cations from aqueous solution, which may in turn provide a strategy for the deposition of active catalysts on the surface of nanotubes [43]. In addition, when nanoparticles and titanate nano- tubes have good electrical contacts, it can provide an efficient interfacial charge- transfer region, which makes this binary system also suitable for photocatalysis. In photo-catalytic processes, the photo sensibilizer could be either wide-bandgap titanate nanotubes [44] or narrow-bandgap semiconductor nanoparticles [45, 46]. At present, these studies are still in the early stages of research, but will undoubtedly find applications in nanofiltration membranes for water treatment.

As in the case of TiO_2 nanotubes, TiO_2 nanorods – as another one-dimensional (1-D) nanostructure – have also been developed for water purification. By using a nonhydrolytic sol–gel reaction between titanium(IV)

iso-propoxide and oleic acid, large-scale TiO_2 nanorods with a narrow distribution of diameters were prepared (see Figure 1) [47]. The anisotropic naked TiO_2 nanorods exhibited a higher photocatalytic activity than the P-25 photocatalyst for the photocatalytic inactivation of E. coli (see Figure 1c).

1.4 TiO_2 Nanofilms

Yu et al. reported that transparent anatase mesoporous TiO2 ($MTiO_2$) and TiO_2 nanometer thin films were prepared on soda-lime glass and fused quartz by the reverse-micelle and sol–gel methods, respectively [48]. $MTiO_2$ thin films showed a higher photocatalytic activity than that of the TiO_2 thin films, because of their higher specific surface areas. Shieh and coworkers developed a new photocatalyst thin film that has strong antibacterial action in visible light [49]. In this study, the radiofrequency (RF) sputter technique was used to deposit a defective titanium dioxide (TiO_2, $x < 2$) photocatalyst thin film on glass and steel substrates. Subsequently, it was demonstrated that the antibacterial performance rate against E. coli could reach 99.99% in visible light.

Furthermore, in order to illustrate the mechanism for the photokilling of E. coli cells on TiO_2 thin film, the survival of intact cells and spheroplasts was investigated as a function of photo-illumination time [50]. Recently, on TiO_2 porous films, attenuated total reflectance (ATR)-FTIR spectroscopy was used to study the pho-tocatalytic peroxidation of E. coli cells, lipopolysaccharide (LPS), phosphatidylethanolamine (PE) and peptidoglycan (PGN) of the E. coli membrane wall [51].

1.5 TiO_2 Nanocomposites

Nanocomposites can combine many advantages from single components. In the case of water treatment, by using conventional grafting, precipitation or impregna-tion, TiO_2 nanoparticles and nanocrystals can be deposited and incorporated to form suitable nanocomposites [52–54]. For example, López-Munoz et al. reported the use of tubular arrays of mesoporous and microporous molecular sieves com- posed of TiO_2 nanoparticles, supported by mesoporous silica, for the water remediation of aromatic pollutants in the presence of UV light [55]. In another report, a novel biocidal photocatalytic nanocomposite, composed of TiO_2 and multi-walled carbon nanotubes (MWNTs) showed a threefold higher photocatalytic specific surface area than commercial TiO_2 nanoparticles (P-25) when dispersed in water. The irradiation of bacterial endospores (Bacillus cereus) with solar UV lamps in the presence of novel photocatalyst led to the successful inactivation of the spores, whereas solar UV lamps only or solar UV lamps with Degussa P-25 showed no significant inactivating behavior [56].

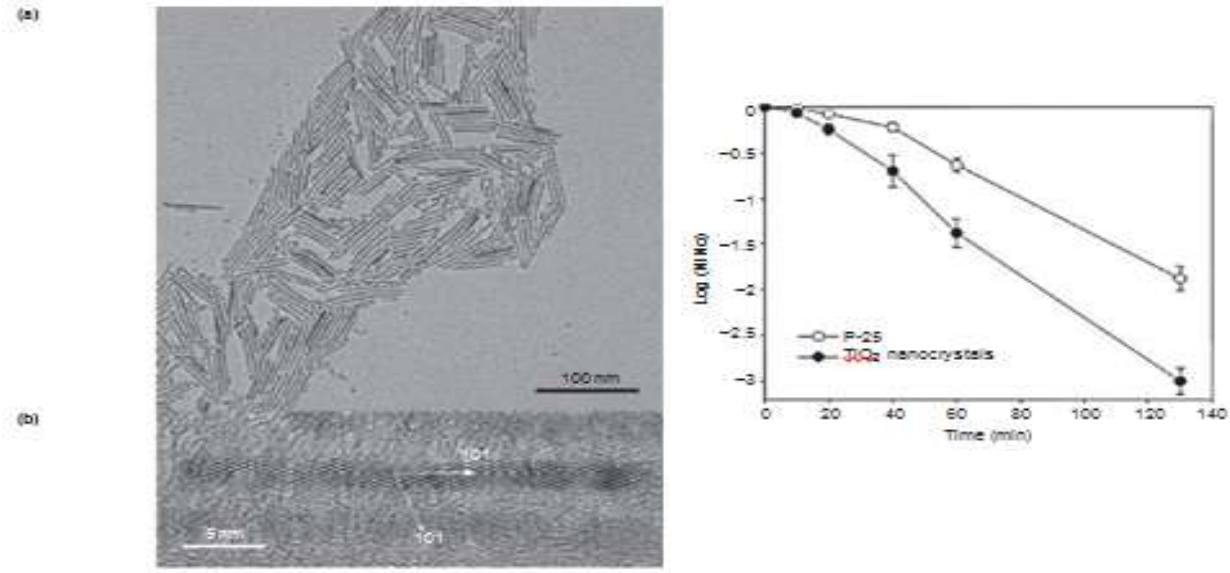

Figure 1. (a) Transmission electron microscopy (TEM) image of as-synthesized TiO_2 nanocrystals; (b) High-resolution (HR) TEM image of TiO_2 nanorods; (c) The photocatalytic inactivation of E. coli using naked TiO_2 nanocrystals and Degussa P-25 as photocatalysts. Reproduced with kind permission from Ref. [47]; © American Chemical Society.

Photocatalysts composed of nanostructured TiO_2 and Fe_2O_3, have also been prepared and used for removal of colored humic acids from wastewater in a UV bubble photocatalytic reactor [57]. Here, Shephard et al. introduced an experimental laboratory-scale 'falling film' reactor which involved TiO_2 nanoparticles for studying the photocatalytic degradation of micro-cystins in aqueous solution [58].

Several methods have been developed to lower the band-gap energy of TiO_2 nanocomposites, examples being sensitizing by dyes or by having semiconductors with lower band-gaps [59]. For instance, Bae et al. reported an example of a visible- light photocatalyst based on TiO_2 modified by ruthenium-complex sensitizers and noble metal deposits such as Pt, Au, Ag and Pd [60]. These authors discussed the effects of metal loading on the visible light activity, and its implications for the efficient visible-light photocatalyst development. CdSe-modified rutile TiO_2 nano- crystals were synthesized by the hydrothermal method, while the photoactivities of the new photocatalyst under visible light illumination were demonstrated by the degradation of methylene blue (MB) [61]. As expected, after sensitization TiO_2 was significantly responsive to visible light illumination, which resulted in the visible light photoactivities increasing. Similarly, nanosized CdS-coupled TiO_2 nanocrystals with an enhanced activity were prepared using a microemulsion- mediated solvothermal method [62]. However, the toxicity and environmental impact was on major concern due to the heavy metal Cd(II) content of these two TiO_2 nanocomposites.

1.6 Iron Oxides

As a typical magnetic material, iron oxides are of major interest in a wide range of fields, including magnetic fluids [63], catalysis [64–66], magnetic resonance imaging (MRI) [67–69], biological cell labeling and sorting [70] and high-density information storage [71]. Whilst many suitable methods such as coprecipitation, thermal decomposition and/or reduction, micelle synthesis and hydrothermal synthesis have been developed for the synthesis of iron oxide nanoparticles, the successful application of such magnetic nanoparticles in these areas is heavily dependent on the stability of the particles under a range of different conditions. Most recently, Lu et al. have reviewed the synthesis, protection, functionalization and application of magnetic nanoparticles (including iron oxides), as well as the magnetic properties of nanostructured systems [72]. However, as yet there are no details of iron oxides nanomaterials being used for applications in water treatment.

Many research groups have used iron oxide nanomaterials, including Fe_2O_3 and Fe_3O_4, as cheap adsorbents to remove toxic ions and organic pollutants from water, and indeed these materials have demonstrated more effective removal capabilities than have bulk materials [73–80]. Typically, Yavuz et al. reported that using the high specific surface area of Fe_3O_4 NCs with a diameter of 12 nm, the mass of waste associated with arsenic was removed from water by orders of magnitude [81]. These processes are often the most effective – or perhaps the only – possible approaches for building a good model quantitatively in water treatment [82]. However, iron oxides were shown to act as low arsenic adsorption capacitor, slow adsorption processes and with narrow optimum pH ranges [83, 84], all of which compromised their applicability. Thus, it is likely that certain protection strategies will be developed, including metal doping, surfactant/polymer coating, silica/ carbon coating and embedding them in a matrix/support [85]. For instance, Zhang et al. reported that Fe oxide materials doped by the metals (Ce, La, Zr) were used for the removal of anions from groundwater [86]. The maximum adsorption capac-ity of the Fe-Ce materials for As (V) ions was significantly higher that of the other adsorbents reported, and the preparation and adsorption properties of the Fe-Ce system have been investigated [87, 88].

Iron oxides nanoparticles with surfaces modified by some photocatalysts, func-tional polymers or special molecules, have also been used as various functional systems for targeted water treatment, including remediation and disinfection. Sun et al. reported a novel photocatalysts composed of nanostructured TiO_2

in the anatase phase, which was uniformly deposited onto porous Fe_2O_3 [89]. The experi-mental results showed the suspended TiO_2/Fe_2O_3 photocatalyst to be effective for the removal of total organic carbon at G1.58% and color400 (i.e. absorbance at 400 nm selected for quantitative analysis of color) at 93.25% at 180 min illumination time, under a 0.4 g l^{-1} catalyst loading and at pH 7.

Poly (1-vinylimidazole) (Im18) with a reactive silane terminal group was grafted directly onto nanosized magnetic particles (maghemite, ç-Fe_2O_3) through siloxane bonds to produce polymer-grafted magnetic nanocomposite particles (Mag-Im18). The Mag-Im18 showed a selective binding of divalent heavy metal ions with a binding strength in the order of $Cu^{2+} > Ni^{2+} > Co^{2+.}$ Selective separation/recovery of Cu^{2+} ions from a Cu^{2+}/Co^{2+} aqueous solution was demonstrated over a pH range of 3 to 7 [90].

Interestingly, based on the high affinity between the bisphosphonate and uranyl ions (due to a chelating effect), Xu group reported that bisphosphonate-modified magnetite nanoparticles could be used to remove the radioactive metal toxins UO^{2+} with high efficiency from water [91]. This simple procedure proved capable of removing 99% of UO^{2+} from the sample. In addition, the principle demonstrated in these studies allowed the detection, recovery and decorporation of other heavy metal toxins from biological systems, either by choosing the ligands or utilizing other novel nanomaterials.

Today, there is a growing threat of water-borne infectious diseases in the developing and developed countries, with E. coli contaminations of food products and Bacillus anthracis attacks frequently reported in recent headline news bulletins. Hence, an urgent task would be to develop effective methods not only for microbial decontamination but also for their rapid detection, without involving time- consuming cell culture. A photokilling approach for pathogenic bacteria was demonstrated using a new type of magnetic nanoprobe which comprised iron oxide/titania (Fe_3O_4@TiO_2) core/shell magnetic nanoparticles as the photokilling agent [92]. This group demonstrated that the IgG-Fe_3O_4@TiO_2 magnetic nanoparticles had the capacity to target several pathogenic bacteria, and could effectively inhibit the cell growth of bacteria targeted by the nanoparticles under irradiation of a low-power UV lamp within a short time period. In another disinfection study, bifunctional Fe_3O_4@Ag nanoparticles with both superparamagnetic and antibacterial properties were prepared by reducing silver nitrate on the surface of Fe_3O_4 nanoparticles using a water-in-oil microemulsion method [93]. The nanoparticles presented a good antibacterial performance against E. coli (Gram-negative bacte-rium), Staphylococcus epidermidis (Gram-positive) and Bacillus subtilis (spores). Moreover, Fe_3O_4@Ag nanoparticles could easily be reclaimed from water by using a magnetic field, thus avoiding any contamination of the surroundings.

Very recently, Huang group developed a magnetic glyco-nanoparticle (MGNP)- based system to rapidly detect E. coli in just 5 min by the unique combination of magnetic nanoparticles and diverse carbohydrate bioactivities [94]. Capture efficiencies achieved were up to 88%, and much higher than the 10–30% range typically observed with antibody- or lectin-functionalized magnetic particles [95, 96]. Moreover, the response patterns of the MGNPs were utilized to explain the pathogen identity for accurately differentiating between three E. coli strains. This was the first time that MGNPs had been used to detect, quantify and differentiate E. coli cells. Decontamination and diagnostic applications can be further developed by this strategy.

Not only zero-dimensional iron oxides nanoparticles can be engineered for water treatment, but novel 3-D or even more complex nanostructures of iron oxides also have excellent abilities to remove heavy metal ions and other pollutants from wastewater. Series of iron oxides with 3-D flowerlike nanostructures have been obtained by a simple calcinations procedure following an ethylene glycol-mediated self-assembly process (see Figure 2) [97]. The nanostructures as-prepared are used to adsorb the As(V), Cr(VI) and Orange II, respectively. The maximum capacity of the α-Fe_2O_3 sample was found to be 7.G mg g1 for As(V), 5.4 mg g^{-1} for Cr(VI) and 43.5 mg g^{-1} for Orange II, which was higher than those of commercial TiO_2 and Fe_2O_3. Moreover, the solid/liquid separation should be straightforward because the sizes of the iron oxide structures were several micrometers (see Table 1 and Figure 3).

1.7 Manganese Oxides

Manganese oxide species (including MnO, Mn_3O_4, Mn_2O_3 and MnO_2) are of considerable importance in technological applications, including molecular adsorption, catalysis and electrochemical supercapacitors,

owing to their structural flexibility combined with novel chemical and physical properties [98–100]. In particular, the many polymorphic forms of manganese dioxide, such as α, β, γ and δ-types, have distinctive properties and now are widely used as ion-sieves and especially as electrode materials in Li/MnO_2 batteries. Bulk MnO_2 and its composites also could be used to remove Cd(II), copper(II), lead(II), uranium(VI), As(III), As(V), Se(IV) and organic waste from water by adsorption and subsequent catalytic combustion at relatively low temperature. During the past few years, various nanostructures of MnO_2, including nanoparticles, nanorods/-belts/-wires/-tubes/-fibers, nanosheets, mesoporous/molecular sieves and branched structures, urchins/orchids and other hierarchical structures, have been synthesized by different methods. However, to our knowledge, there are few reports in existence concerning the MnO_2 nanostructures used in water treatment.

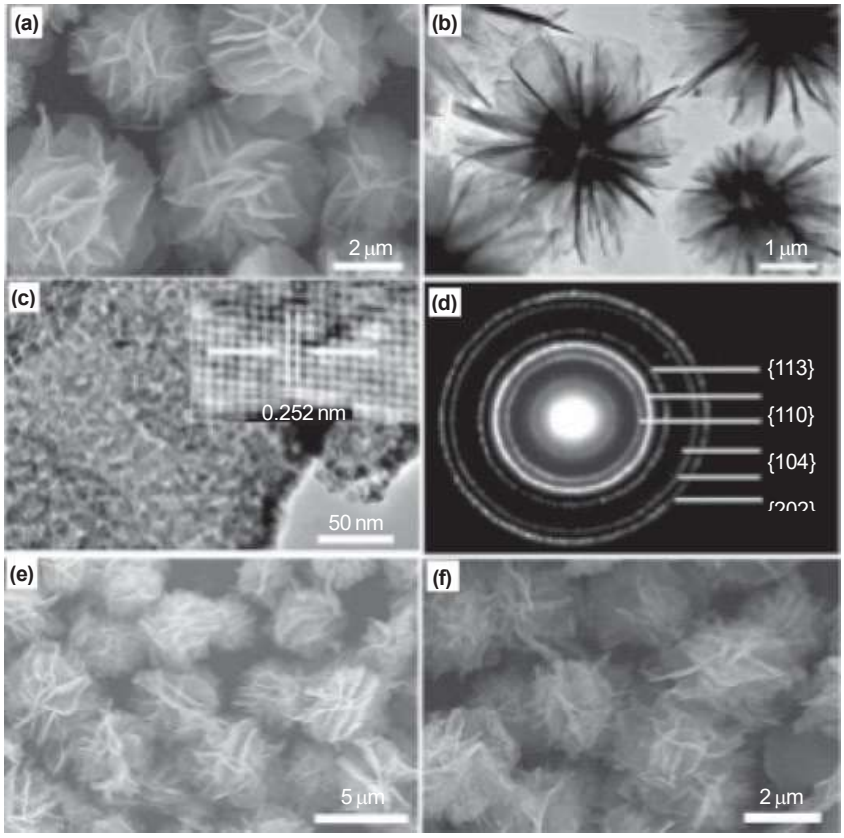

Figure 2. (a) Scanning electron microscopy (SEM) and (b) TEM images of the as-obtained α-Fe_2O_3; (c) High-magnification TEM image of the petal of the flower-like structure of the as-obtained α-Fe2O3. Inset: High-resolution TEM (HRTEM) image taken from the (d) Selected-area electron diffraction (SAED) pattern of the as-obtained α-Fe_2O_3; (e) SEM image of the as-obtained Fe_3O_4; (f) SEM image of the as-obtained α-Fe_2O_3. Reproduced with kind permission from Ref. [97]; © John Wiley & Sons, Inc. as-obtained α-Fe_2O_3 nanoparticle;

Absorbent sample	BET surface area (m^2 g^{-1})	Removal capacity for As (mg g^{-1})	Removal capacity for Cr (mg g^{-1})
α-Fe_2O_3	40	5.31	4.47
α-Fe_2O_3	56	4.75	3.86
Fe_3O_4	34	4.65	4.38
Commercial -Fe_2O_3	2	0.46	0.68
Commercial TiO_2	45	4.11	2.42

Table 1: BET surface area and removal capacity of different types of adsorbent sample. The initial

concentration of both As(V) and Cr(VI) was 10.63 mg $^{-1}$. Reproduced with kind permission from Ref. [97]; © John Wiley & Sons, Inc.

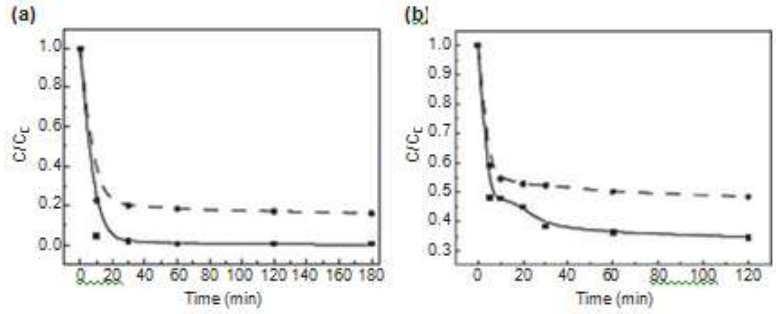

Figure 3. (a) Adsorption rate of As(V) (solid line) and Cr(VI) (dashed line) on the as-prepared α-Fe_2O_3; (b) Adsorption rate of the azo-dye Orange II on new as-prepared α-Fe_2O_3 (solid line) and regenerated α -Fe_2O_3 (dashed line). Reproduced with kind permission from Ref. [97]; © John Wiley & Sons, Inc.

Among the anisotropic nanostructures, 1-D nanostructures appear as an exciting research field for the great potential of addressing space-confined transport phenomena, as well as applications. ®–MvO2 has been used as a catalyst for H_2O_2 decomposition, which would assist when taking advantage of this process to accelerate the decoloration and mineralization of organic dyes. Recently, Zhang et al. reported that ®–MvO2 nanorods have been synthesized by the thermal decomposition of a template precursor of MnOOH, which was obtained by hydrothermal treatments of $KMnO_4$ in an aqueous ethanol solution (Figure 4). As shown in Figure 9.5, the catalytic activity is much higher than that of commercial microsized MnO_2 powders, due to the larger surface area and more active surface sites of the ®–MvO2 nanorods.

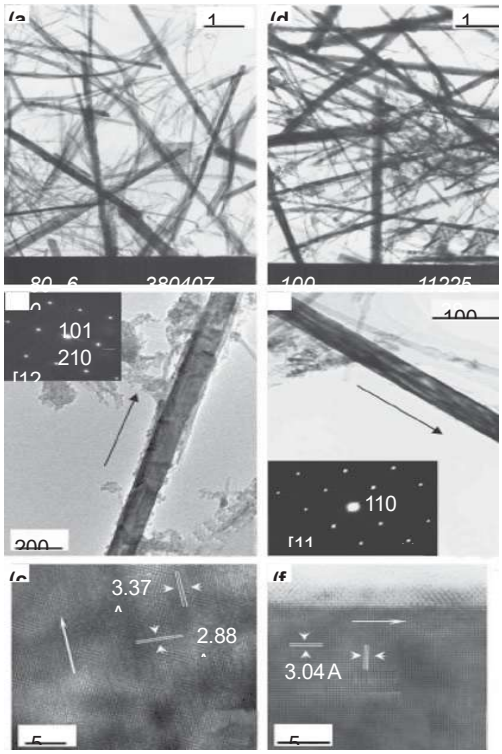

Figure 4. TEM/HRTEM images or SAED patterns. (a) MnOOH nanorods; (b) A single MnOOH nanorod (inset: SAED pattern); (c) MnOOH nanorod (HRTEM); (d) ®–MvO2nanorods; (E) A single ®–MvO2nanorod (inset: SAED pattern); (f) ®–MvO2nanorod (HRTEM). Reproduced from Ref.; © Elsevier B.V.

International Journal of Environmental Sciences
ISSN: 2229-7359
Vol. 11 No. 8s, 2025
https://www.theaspd.com/ijes.php

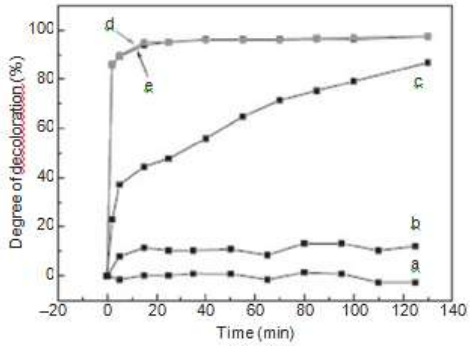

Figure 5. Time profiles of methylene blue (MB) degradation.
(a) MB+H_2O_2;(b)MB+®–Mvo2 nanorods; (c)MB + H_2O_2 + commercial ®–Mvo2powder; (d) MB+ H_2O_2 + MnO_2 nanorods; (e) MB + H_2O_2 + ®–Mvo2nanorods (dark). Reproduced with kind permission from Ref; © Elsevier B.V.

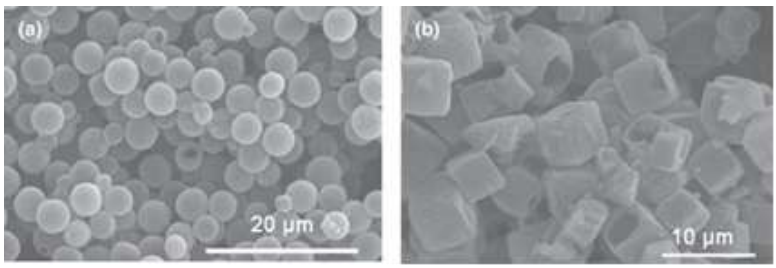

Figure 6. The SEM images of (a) MnO_2 microspheres and (b)MnO_2 microcubes. Reproduced with kind permission from Ref.; © John Wiley & Sons, Inc.

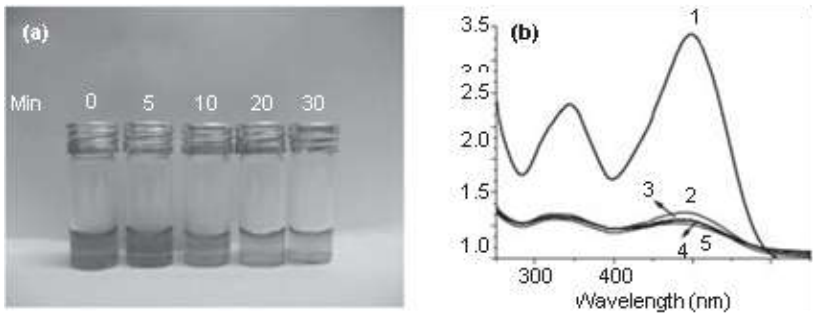

Figure 7. (a) Absorption of Congo red with time by new MnO_2 microspherical hollow hierarchical nanostructures; (b) Absorption spectra of a solution of Congo red (100 mg $^{-1}$, 20 ml) in the presence of MnO_2 hierarchical hollow microspheres (0.03 g) at different time intervals (min) of: (1) 0; (2) 5; (3) 10; (4) 20; and (5) 30. Reproduced with kind permission from Ref.; © John Wiley & Sons, Inc.

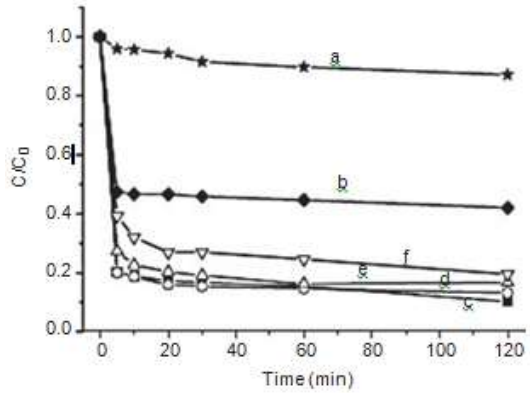

Figure 8. Adsorption rate of the azo-dye Congo red on (a) commercial MnO_2; (b) commercial γ-Fe_2O_3; (c) new as-prepared MnO_2 hierarchical hollow microspheres; (d) secondary; (e) third; and (f) fourth regenerated

particles. C0 (mg $^{-1}$) is the initial concentration of the Congo red solution; C (mg $^{-1}$) is the dye concentration at different intervals during the adsorption. Reproduced with kind permission from Ref.; © John Wiley & Sons, Inc.

More recently, our group has shown that MnO_2 with intricate and well- controlled 3-D morphologies are synthesized by combining the Kirkendall effect with a sacrificial crystalline template. In detail, the hierarchical hollow manganese dioxide can be successfully synthesized by shape-preserving $KMnO_4$ oxidation of micrometer-scale manganese carbonate structures at room temperature, followed by the selective removal of $MnCO_3$ with HCl. This created a novel route to the synthesis of MnO_2 superstructures with unique morphologies and complex hierarchies at the microscale and nanoscale. Based on the novel nanostructures, the as-prepared MnO_2 nanomaterials were used as an adsorbent for the removal of organic pollutant in waste water (see Figure 6). Based on the data shown in Figures 7 and 8, the maximum adsorption capacitor of the nanostructures is about 60 mg g1 for Congo red, which is higher than those of commercial micro- sized MnO_2 and γ-Fe_2O_3 with an average size of 20–30 nm. This might be ascribed to the special hierarchical hollow microstructure of as-obtained MnO_2, which pro- vided a new and more efficient material for applications in organic wastewater treatment. After adsorption, the solid–liquid separation can be achieved very easily because of the relatively higher density, while the MnO_2 nanostructures in water treatment can be reused many times.

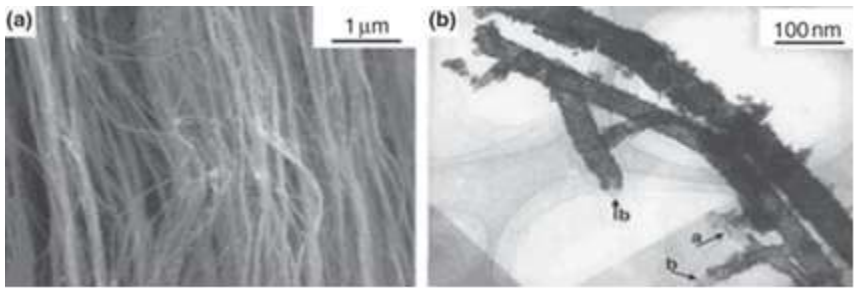

Figure 9. a) SEM images of aligned carbon nanotubes (ACNTs); (b) TEM image of CeO_2/ACNTs. Reproduced with kind permission from Ref. [164]; © Elsevier B.V.

1.8 Cerium Oxide (CeO_2)

Hydrous rare earth oxides have been proposed as a new adsorbent for the removal of aqueous hazardous anions such as arsenate, fluoride and phosphate, because of their relatively higher adsorption capacitors. The relatively small ionic potential and strong basicity of rare earth ions bring a strong tendency to dissociate OH groups into hydroxyl ions . As a typical form of rare earth oxide, ceria has been given wide attention because of its unique physical and chemical properties, including oxygen ion conductivity and oxygen storage capacity. Because of these characteristics, ceria has been widely used for fuel cell, sensor and chemical–mechanical polishing for microelectronics, phosphor/luminescence and catalysts. Until now, the various nanostructures of ceria such as nanoparticles, nanorods/ nanowires/ nanotubes [160–162] and nano-polyhedrons have been synthesized using different methods. However, the application of ceria nano- structures for water treatment is rare, mainly because of the high costs involved when using rare earth compounds. Many research groups have attempted to develop new adsorbents with a high adsorption capacity and relatively low cost. For example, cerium oxide nanoparticles supported on carbon nanotubes (CeO2- CNT) or on aligned carbon nanotubes (CeO_2-ACNTs) have been developed as effective adsorbents for As(V) (see Figure 9). Surprisingly, correct addition of the divalent cations Ca(II) and Mg(II) was found to increase the amount of adsorbed As(V), from 10 to 82 mg g1. The largest Cr(VI) adsorption capacity was 30.2 mg g1 at pH 7.0, which was twofold higher than those of activated carbon and $Al2O_3$ (see Figure 10).

Novel nanostructures can expand the advanced applications of nanomaterials. More recently, Wan and coworkers showed that the as-prepared ceria 3-D nano- material could be used as a good adsorbent for the removal of As(V) and Cr(VI) in wastewater treatment (Figure 11). The maximum adsorption capacity of the ceria as-prepared was found to be 14.4 mg g1 for As(V) and 5.9 mg g1 for Cr(VI), respectively. After

adsorption, the solid/liquid separation in suspension was performed very easily by using centrifugation. Moreover, this new adsorbent could be recovered and reused, which proved to be very useful for real applications when cutting operational costs. The main advantages of the 3-D nanostructure, which it was claimed made CeO_2 particularly attractive for environmental remediation and other applications, were that: (i) separation and recycle were easier com- pared with common nanoparticles, as the total size of the structure was on the micrometer scale; (ii) the as-obtained CeO_2 retained a high specific surface area as the micropetal of the composite structure was composed of interconnected nanoparticles; and (iii) the flowerlike structure could effectively prevent further aggregation, so that an unblocked mass transfer and high catalytic activity could be retained.

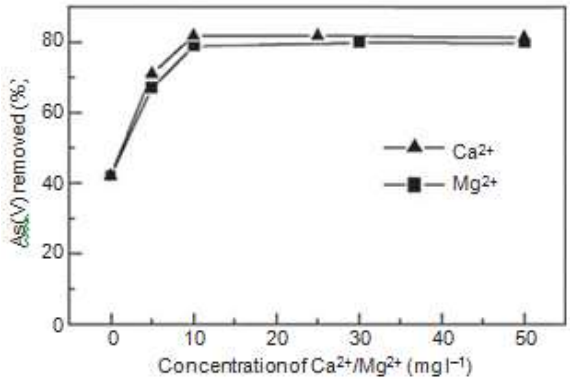

Figure 10. The effect of Ca_2+ and Mg_2+ on adsorption (C0 = 20 mg l□1; m = 0.025 g; t = 24 h). Reproduced with kind permission from Ref.; © Elsevier B.V.

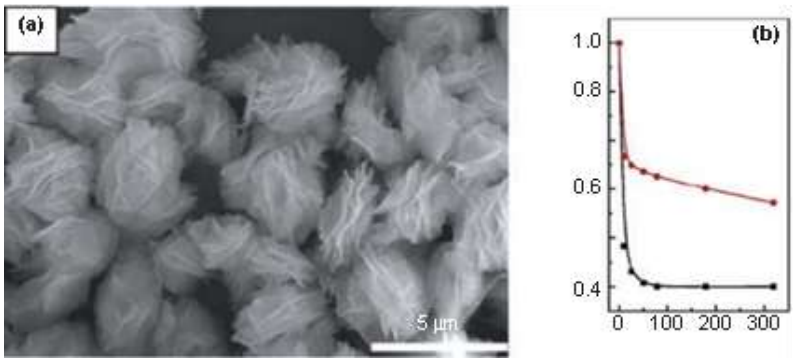

Figure 11. (a) SEM image of the as-obtained ceria; (b) Adsorption rate of As(V) (black line, initial concentration of 12.9 mg g^{-1}) and Cr(VI) (red line, initial concentration of 17.2 mg g^{-1}) on the as-prepared ceria. Reproduced with kind permission from Ref.; © American Chemical Society.

1.9 Magnesium Oxide (MgO)

As far as magnesium oxide (MgO) is concerned, very few reports have been made to date regarding the use of its nanostructures for water treatment. Stoimenov et al. reported that reactive magnesium oxide nanoparticles and halogen (Cl_2, Br_2) adducts of the MgO particles were prepared to contact certain bacteria and spore cells. Bacteriological test data subsequently showed that these materials were very effective against Gram-positive Staphylococcus aureus and Gram-negative E. coli, Klebsiella pneumoniae and Pseudomonas aeruginosa) bacteria, as well as spores. It was suggested that the material's abrasiveness, basic character, electrostatic attraction and oxidizing power (due to the presence of active halogen) combine to promote these biocidal properties. Subsequently, Koper and co-workers described the size effect of the antibacterial activities of MgO nanoparticles. More details indicated that smaller MgO nanoparticles with a diameter of 8 nm had the highest activity in killing E. coli and S. aureus, while a gradual decrease in antibacterial activity was observed with increase in particle size (from 11 to 23 nm).

Alumina (Al_2O_3)

Membrane processes are considered as important components of advanced water purification and desalination technologies. Alumina (Al_2O_3) nanoparticles, when used as robust ceramic membranes for supporting functional substances, are applied for water treatment. In recent years, several reactive and functionalized Al_2O_3 membranes have been developed for use in water filtration processes. For example, when using alumina (A-alumoxane) nanoparticles, DeFriend et al. reported the fabrication of alumina ultrafilter (UF) membranes which showed selectivity toward three different synthetic dyes. By using a layer-by-layer technique, positive poly(allylamine hydrochloride) (PAH) and negative poly(styrene sulfonate) (PSS) were assembled onto porous alumina for the fabrication of novel nanofilter (NF) membranes. These NF membranes exhibited a high water flux, a high retention of divalent cations (Ca_2+ and Mg_2+), and Cl^-/ SO^{2-} selectivity ratios of up to 80. Moreover, based on the good catalysis of gold nanoparticles, through layer-by-layer adsorption of polyelectrolytes and citrate-stabilized gold nanoparticles, a composite membrane composed of alumina and polymers was prepared by Dotzauer et al. The result in this study showed that the mem- branes could reduce more than 99% of 0.4% mM 4-nitrophenol to 4-aminophenol. Such studies have been extended through the use of ceramic membranes made from alumina (Al_2O_3) impregnated with crosslinked, silylated dendritic or cyclodextrin polymers.

Pd-Cu/γ-alumina, a bimetallic active catalyst, was prepared for the reduction of NO. It should be noted here that this design can be regarded as one of the futuristic remediation strategies for mineralizing the brine, because this nanocom-posite can convert organic compounds into innocuous N_2 without any deleterious brine.

Conventional activated alumina (AA) has certain disadvantages, including ill- defined pore structures, low adsorption capacities and subsequently slow kinetics. In order to overcome these difficulties, through a post-hydrolysis, mesoporous alumina (MA) with a large surface area and uniform pore size was prepare arsenic removal. The maximum As(V) uptake by MA was sevenfold higher (121 mg of As(V) g^{-1} and 47 mg of As(III) g^{-1}) than that of conventional AA. Mean- while, more than 85% of the adsorbed arsenic could be desorbed in less than 1 h using 0.05 M NaOH. Thus, it was suggested that MA, as-prepared, could be easily reusable and reclaimable.

In addition, as a relatively mature technique, Al_2O_3 nanomembranes can be obtained by electrochemical anodic oxidation, and their thicknesses, pore diameters and densities adjusted by operational conditions such as electrolytes, voltages and temperatures. Under the assistance of porous aluminum, nanowires, nano- tubes and more complex nanostructures can be prepared controllably , and this may open the door to the preparation of functional anisotropic NF membranes for high throughput in real applications.

2. SUMMARY

Water has a major impact on every facet of human activity, including health, energy and food production, industrial output and the quality of the environment. In recent years, as a result of extended droughts, population growth, more stringent health-based regulations and increasing demands from a variety of users, water is today becoming a competitive resource – indeed, in many parts of the world it is regarded as the 'oil of the twenty-first century'. Metal oxide nanomaterials have many important physico-chemical and biological properties that make them particularly attractive for water treatment. Due to their large surface areas and their size-, shape- and dimension-dependent catalytic properties, considerable efforts have driven exploration into the uses of metal oxide nanomaterials for applications such as catalysis, adsorption and membrane separations. In addition, metal oxide nanomaterials can be functionalized with various chemical groups to increase their affinity towards many interesting compounds. This may result in ligands that are not only recyclable but also have a high capacity and selectivity for toxic metal ions and inorganic anions, as well as for bacteria and viruses in aqueous solutions. Today, we envision metal oxide nanomaterials as being engineered to remove current and emerging pathogens without any toxic byproducts, to realize targeted sensing and detection, transformation and the removal of low- concentration or trace contaminations in high backgrounds at lower cost, and to be reusable, reclaimable and recyclable.

It is, therefore, very important that a systematic overview of water treatments be undertaken since, even when efficient metal oxide nanomaterials have been prepared for the treatment of water it is also vital to consider the subject from an engineering aspect. Indeed, in some cases this may be more important than the unique nature of the materials themselves. Likewise, it should be noted – from a precautionary angle – that the very properties of these nanomaterials which render them attractive for water treatment might also cause them to become eco-toxic.

Based on this review paper we can conclude that the nano metal oxides of TiO_2 and FeO_2 is more efficient for water purification process. Despite the widespread use of titanium dioxide (TiO_2) in photocatalytic applications, its inherent limitations, such as low efficiency under visible light and rapid recombination of electron-hole pairs, hinder its effectiveness in environmental remediation. If ingested, FeO2 in water usually has no direct health risks. This review paper including TiO_2, MgO, MnO, Al_2O_3 aiming to assess their potential for enhancing photocatalytic applications. Photocatalysis holds promise in environmental remediation, water purification, and energy conversion, with TiO_2&FeO_2 being a prominent photocatalyst.

REFERENCES

[1.] Schwarzenbach, R.P., Escher, B.I., Fenner, K., Hofstetter, T.B., Johnson, C.A., Gunten, U.V. and Wehrli, B. (2006) The challenge of micropollutants in aquatic systems. Science, 303, 1072–7.

[2.] Shannon, M.A., Bohn, P.W., Elimelech, M., Georgiadis, J.G., Marina, B.J. and Mayers, A.M. (2008) Science and technology for water purification in the coming decades. Nature, 452, 301–10.

[3.] Theron, J., Walker, J.A. and Cloete, T.E. (2008) Nanotechnology and water treatment: applications and emerging opportunities. Critical Reviews in Microbiology, 34, 43–G9.

[4.] Fujishima, A. and Honda, K. (1972) Electrochemical photolysis of water at a semiconductor electrode. Nature, 238, 37–8.

[5.] Linsebigler, A.L., Lu, G. and Yates, J.T. (1995) Photocatalysis on TiO2 surfaces: principles, mechanisms, and selected results. Chemical Reviews, 95, 735–58.

[6.] Zhang, Z., Wang, C.C., Zakaria, R. and Ying, J.Y. (1998) Role of particle size in nanocrystalline TiO2-based photocatalysts. Journal of Physical Chemistry B, 102, 10871–8.

[7.] Rao, C.N.R., Kulkarni, G.U., Thomas, P.J. and Edwards, P.P. (2002) Size-dependent chemistry: properties of nanocrystals. Chemistry – A European Journal, 8, 28–35.

[8.] Amal, R., McEvoy, S., Beydoun, D. and Low, G. (1999) Role of nanoparticles in photocatalysis. Journal of Nanoparticle Research, 1, 439–58.

[9.] Ohno, T., Sarukawa, K., Tokieda, K. and Matsumura, M. (2001) Morphology of a TiO2 photocatalyst (Degussa P-25) consisting of anatase and rutile crystalline phases. Journal of Catalysis, 203, 82–G.

[10.] Zhang, J., Xu, Q., Feng, Z.C., Li, M.J. and Li, C. (2008) Importance of the relationship between surface phases and photocatalytic activity of TiO2. Angewandte Chemie – International Edition, 47, 17GG–9.

[11.] Prieto, O., Fermoso, J., Nuez, Y., Del Valle, J.L. and Irusta, R. (2005) Decoloration of textile dyes in wastewaters by photocatalysis with TiO2. Solar Energy, 79, 37G–83.

[12.] Liu, Z., He, Y., Li, F. and Liu, Y. (2006) Photocatalytic treatment of RDX wastewater with nano-sized titanium dioxide. Environmental Science and Pollution Research International, 13, 328–32.

[13.] Dvoranova, D., Brezova, V. and Malati, M.A. (2002) Investigations of metal-doped titanium dioxide photocatalysts. Applied Catalysis B: Environmental, 37, 91–105.

[14.] Yang, M.C., Yang, T.S. and Wong, M.S. (2004) Nitrogen-doped titanium oxide films as visible light photocatalyst by vapor deposition. Thin Solid Films, 469, 1–5.

[15.] Ohno, T., Mitsui, T. and Matsumura, M. (2003) Photocatalytic activity of S-doped photocatalyst under visible light. Chemistry Letters, 32, 3G4–5.

[16.] Hirano, K., Suzuki, E., Ishikawa, A., Moroi, T., Shiroishi, H. and Kaneko, M. (2000) Sensitization of TiO2 particles by dyes to achieve H2 evolution by visible light. Journal of Photochemistry and Photobiology A: Chemistry, 136, 157–G1.

[17.] Irie, H., Watanabe, Y. and Hashimoto, K. (2003) Carbon-doped anatase as a visible light-sensitive photocatalyst. Chemistry Letters, 32, 772–3.

[18.] Liu, Y., Li, J., Qiu, X. and Burda, C. (2006) Novel TiO2 nanocatalysts for wastewater purification – tapping energy from the sun. Water Practice and Technology, 1 doi: 10.21GG/wpt.2006.073.

[19.] Nahar, S., Hasegawa, K. and Kagaya, S. (2006) Photocatalytic degradation of phenol by visible light-responsive iron-doped TiO2 and spontaneous sedimentation of the TiO2 particles. Chemosphere, 65, 197G–82.

[20.] Oh, S.M., Kim, S.S., Lee, J.E., Ishigaki, T. and Park, D.W. (2003) Effect of additives on photocatalytic activity of titanium dioxide powders synthesized by thermal plasma. Thin Solid Films, 435, 252–8.
[21.] Barakat, M.A., Schaeffer, H., Hayes, G. and Ismat-Shah, S. (2005) Photocatalytic degradation of 2-chlorophenol by Co-doped TiO2 nanoparticles. Applied Catalysis B: Environmental, 57, 23–30.
[22.] Chiou, C.H. and Juang, R.S. (2007) Photocatalytic degradation of phenol in aqueous solutions by Pr-doped TiO2 nanoparticles. Journal of Hazardous Materials, 149, 1–7.
[23.] Shah, S.I., Li, W., Huang, C.P., Jung, O. and Ni, C. (2002) Study of Nd3+, Pd2+, Pt4+ and Fe3+ dopant effect on photoreactivity of TiO2 nanoparticles. Proceedings of the National Academy of Sciences of the United States of America, 99, G482–G.
[24.] Pena, M.E., Korfiatis, G.P., Patel, M., Lippincott, L. and Meng, X. (2005) Adsorption of As(V) and As(III) by nanocrystalline titanium dioxide. Water Research, 39, 2327–37.
[25.] Jiang, F., Zheng, Z., Xu, Z., Zheng, S., Guo, Z. and Chen, L. (2006) Aqueous Cr(VI) photo-reduction catalyzed by TiO2 and sulfated TiO2. Journal of Hazardous Materials, 134, 94–103.
[26.] Wei, C., Lin, W.Y., Zainal, Z., Nathan, T., Williams, E., Zhu, K., Krurlc, A.P., Smith, R.L. and Rajeshwar, K. (1994) Bactericidal activity of TiO2 photocatalyst in aqueous media: toward a solar-assisted water disinfection system. Environmental Science & Technology, 28, 934–8.
[27.] Bekbolet, M. and Araz, C. (199G) Inactivation of Escherichia coli by photocatalytic oxidation. Chemosphere, 32, 959–G5.
[28.] Maness, P.-C., Smolinski, S., Blake, D.M., Huang, Z., Wolfrum, E.J. and Jacoby, W.A. (1999) Bactericidal activity of photocatalytic TiO2 reaction: toward an understanding of its killing mechanism. Applied and Environmental Microbiology, 65, 4094–8.
[29.] Yu, J.C., Ho, W., Yu, J., Yip, H., Wong, P.K. and Zhao, J. (2005) Efficient visible light-induced photocatalytic disinfection on sulfur-doped nanocrystalline titania. Environmental Science & Technology, 39, 1175–9.
[30.] Egerton, T.A., Kosa, S.A. and Christensen, P.A. (2006) Photoelectrocatalytic disinfection of E. coli suspensions by iron doped TiO2. Physical Chemistry Chemical Physics: PCCP, 8, 398–40G.
[31.] Bavykin, D.V., Gordeev, S.N., Moskalenko, A.V., Lapkin, A.A. and Walsh, F.C. (2005) Apparent two-dimensional behavior of TiO2 nanotubes revealed by light absorption and luminescence. Journal of Physical Chemistry B, 109, 85G5–9.
[32.] Sakai, N., Ebina, Y., Takada, K. and Sasaki, T. (2004) Electronic band structure of titania semiconductor nanosheets revealed by electrochemical and photoelectrochemical studies. Journal of the American Chemical Society, 126, 5851–8.
[33.] Kasuga, T., Hiramatsu, M., Hoson, A., Sekino, T. and Niihara, K. (1998) Formation of titanium oxide nanotube. Langmuir, 14, 31G0–3.
[34.] Sander, M.S., Coete, M.J., Gu, W., Kile, B.M. and Tripp, C.P. (2004) Template-assisted fabrication of dense, aligned arrays of titania nanotubes with well-controlled dimensions on substrates. Advanced Materials, 22, 2052–7.
[35.] Gong, D., Grimes, C.A., Varghese, O.K., Hu, W., Singh, R.S., Chen, Z. and Dickey, E.C. (2001) Titanium oxide nanotube arrays prepared by anodic oxidation. Journal of Materials Research, 16, 3331–4.
[36.] Bavykin, D.V., Friedrich, J.M. and Walsh, F.C. (2006) Protonated titanates and TiO2 nanostructured materials: synthesis, properties, and applications. Advanced Materials, 18, 2807–24.
[37.] Adachi, M., Murata, Y., Okada, I. and Yoshikawa, S. (2003) Formation of titania nanotubes and applications for dye-sensitized solar cells. Journal of the Electrochemical Society, 150, G488.
[38.] Ngamsinlapasathian, S., Sakulkhaemaruethai, S., Pavasupree, S., Kitiyanan, A., Sreethawong, T., Suzuki, Y. and Yoshikawa, S. (2004) Highly efficient dye-sensitized solar cell using nanocrystalline titania containing nanotube structure. Journal of Photochemistry and Photobiology A, 164, 145–51.
[39.] Varghese, O.K., Gong, D., Paulose, M., Ong, K.O., Dickey, E.C. and Grimes, C.A. (2003) Extreme changes in the electrical resistance of titania nanotubes with hydrogen exposure. Advanced Materials, 15, G24–7.
[40.] Mor, G.K., Carvalho, M.A., Varghese, O.K., Pishko, M.V. and Grimes, C.A. (2004) A room temperature TiO2-nanotube hydrogen sensor able to self-clean photoactively from environmental contamination. Journal of Materials Research, 19, G28–34.
[41.] Mor, G.K., Shankar, K., Paulose, M., Varghese, O.K. and Grimes, C.A. (2005) Enhanced photocleavage of water using titania nanotube arrays. Nano Letters, 5, 191–5.
[42.] Chen, Y., Crittenden, J., Hackney, S., Sutter, L. and Hand, D. (2005) Preparation of a novel TiO2-based p-n junction nanotube photocatalyst. Environmental Science & Technology, 39, 1201–8.
[43.] Bavykin, D.V., Lapkin, A.A., Plucinski, P.K., Torrente-Murciano, L., Friedrich, J.M. and Walsh, F.C. (2006) Deposition of Pt, Pd, Ru and Au on the surfaces of titanate nanotubes. Topics in Catalysis, 39, 151–G0.

[44.] Lin, C.H., Lee, C.H., Chao, J.H., Kuo, C.Y., Cheng, Y.C., Huang, W.N., Chang, H.W., Huang, Y.M. and Shih, M.K. (2004) Photocatalytic generation of H2 gas from neat ethanol over Pt/TiO2 nanotube catalysts. Catalysis Letters, 98, G1–G.

[45.] Cao, J., Sun, J.Z., Li, H.Y., Hong, J. and Wang, M. (2004) A facile room-temperature chemical reduction method to TiO2@CdS core/sheath heterostructure nanowires. Journal of Materials Chemistry, 14, 1203–G.

[46.] Hodos, M., Horvath, E., Haspel, H., Kukovecz, A., Konya, Z. and Kiricsi, I. (2004) Photosensitization of ion-exchangeable titanate nanotubes by CdS nanoparticles. Chemical Physics, 399, 512–15.

[47.] Joo, J., Kwon, S.G., Yu, T., Cho, M., Lee, J., Yoon, J. and Hyeon, T. (2005) Large-scale synthesis of TiO2 nanorods via nonhydrolytic sol-gel ester elimination reaction and their application to photocatalytic inactivation of E. coli. The Journal of Physical Chemistry B, 109, 15297–302.

[48.] Yu, J.C., Yu, J.G. and Zhao, J.C. (2002) Enhanced photocatalytic activity of mesoporous and ordinary TiO2 thin films by sulfuric acid treatment. Applied Catalysis B: Environmental, 36, 31–43.

[49.] Shieh, K.J., Li, M., Lee, Y.H., Sheu, S.D., Liu, Y.T. and Wang, Y.C. (2006) Antibacterial performance of photocatalyst thin film fabricated by defection effect in visible light. Nanomedicine: Nanotechnology, Biology and Medicine, 2, 121–G.

[50.] Sunada, K., Watanabe, T. and Hashimoto, K. (2003) Studies on photokilling of bacteria on TiO2 thin film. Journal of Photochemistry and Photobiology A: Chemistry, 156, 227–33.

[51.] Kiwi, J. and Nadtochenko, V. (2005) Evidence for the mechanism of photocatalytic degradation of the bacterial wall membrane at the TiO2 interface by ATR-FTIR and laser kinetic spectroscopy. Langmuir, 21, 4G31–41.

[52.] Tuel, A. and Hubert-Pfalzgraf, L.G. (2003) Nanometric monodispersed titanium oxide particles on mesoporous silica: synthesis, characterization, and catalytic activity in oxidation reactions in the liquid phase. Journal of Catalysis, 217, 343–53.

[53.] Reddy, M.P., Venugopal, A. and Subrahmanyam, M. (2007) Hydroxyapatite-supported Ag-TiO2 as Escherichia coli disinfection photocatalysts. Water Research, 41, 379–8G.

[54.] Zhang, X., Zhang, F. and Chan, K.Y. (2005) Synthesis of titania-silica mixed oxide mesoporous materials, characterization and photocatalytic properties. Applied Catalysis A, 284, 193–8.

[55.] López-Munoz, M.J., Van Grieken, R., Aguado, J. and Marugán, J. (2005) Role of the support on the activity of silica-supported TiO2 photocatalysts: structure of the TiO2/SBA-15 photocatalysts. Catalysis Today, 101, 307–14.

[56.] Lee, S.H., Pumprueg, S., Moudgil, B. and Sigmund, W. (2005) Inactivation of bacterial endospores by photocatalytic nanocomposites. Colloids and Surfaces B: Biointerfaces, 40, 93–8.

[57.] Qiao, S., Sun, D.D., Tay, J.H. and Easton, C. (2003) Photocatalytic oxidation technology for humic acid removal using a nano-structured TiO2/Fe2O3 catalyst. Water Science and Technology, 47, 211–17.

[58.] Shephard, G.S., Stockenstrom, S., de Villiers, D., Engelbrecht, W.J. and Wessels, G.F.S. (2002) Degradation of microcystin toxins in a falling film photocatalytic reactor with immobilized titanium dioxide catalyst. Water Research, 36, 140–G.

[59.] Wu, L., Yu, J.C. and Fu, X.Z. (2006) Characterization and photocatalytic mechanism of nanosized CdS coupled TiO2 nanocrystals under visible light irradiation. Journal of Molecular Catalysis A: Chemical, 244, 25–32.

[60.] Bae, E. and Choi, W. (2003) Highly enhanced photoreductive degradation of perchlorinated compounds on dye-sensitized metal/TiO2 under visible light. Environmental Science & Technology, 37, 147–52.

[61.] Liu, H.Y. and Gao, L. (2005) Synthesis and properties of CdSe-sensitized rutile TiO2 nanocrystals as a visible light-responsive photocatalyst. Journal of the American Ceramic Society, 88, 1020–2.

[62.] Yu, J.C., Wu, L., Lin, J., Li, P. and Li, Q. (2003) Microemulsion-mediated solvo-thermal synthesis of nanosized CdS-sensitized TiO2 crystalline photocatalyst. Chemica Communications, 8, 1552–3.

[63.] Chikazumi, S., Taketomi, S., Ukita, M., Mizukami, M., Miyajima, H., Setogawa, M. and Kurihara, Y. (1987) Physics of magnetic fluids. Journal of Magnetism and Magnetic Materials, 65, 245–51.

[64.] Lu, A.H., Schmidt, W., Matoussevitch, N., Bennermann, H., Spliethoff, B., Tesche, B., Bill, E., Kiefer, W. and Schüth, F. (2004) Nanoengineering of a magnetically separable hydrogenation catalyst. Angewandte Chemie – International Edition, 43, 4303–G.

[65.] Tsang, S.C., Caps, V., Paraskevas, I., Chadwick, D. and Thompsett, D. (2004) Magnetically separable, carbon-supported nanocatalysts for the manufacture of fine chemicals. Angewandte Chemie – International Edition, 43, 5G45–9.

[66.] Shokouhimehr, M., Piao, Y.Z., Kim, J.Y., Jang, Y.J. and Hyeon, T. (2007) A magnetically recyclable nanocomposite catalyst for olefin epoxidation. Angewandte Chemie – International Edition, 46, 7039–43.

[67.] Gupta, A.K. and Gupta, M. (2005) Synthesis and surface engineering of iron oxide nanoparticles for biomedical applications. Biomaterials, 26, 3995–4021.

[68.] Mornet, S., Vasseur, S., Grasset, F., Verveka, P., Goglio, G., Demourgues, A., Portier, J., Pollert, E. and Duguet, E. (2006) Magnetic nanoparticle design for medical applications. Progress in Solid State Chemistry, 34, 237–47.
[69.] Li, Z., Wei, L., Gao, M.Y. and Lei, H. (2005) One-pot reaction to synthesize biocompatible magnetite nanoparticles. Advanced Materials, 17, 1001–5.
[70.] Chemla, Y.R., Grossman, H.L., Poon, Y., McDermott, R., Stevensi, R., Alper, M.D. and Clarke, J. (2000) Ultrasensitive magnetic biosensor for homogeneous immunoassay. Proceedings of the National Academy of Sciences of the United States of America, 97, 142G8–72.
[71.] Hyeon, T. (2003) Chemical synthesis of magnetic nanoparticles. Chemical Communications, 927–34.
[72.] Lu, A.H., Salabas, E.L. and Schüth, F. (2007) Magnetic nanoparticles: synthesis, protection, functionalization, and application. Angewandte Chemie – International Edition. 46, 1222–44.
[73.] Li, P., Miser, D.E., Babier, S., Yadav, R.T. and Hajaligol, M.R. (2003) The removal of carbon monoxide by iron oxide nanoparticles. Applied Catalysis B, 43, 151–G2.
[74.] Oliveira, L.C.A., Petkowicz, D.I., Smaniotto, A. and Pergher, S.B.C. (2004) Magnetic zeolites: a new adsorbent for removal of metallic contaminants from water. Water Research, 38, 3G99–704.
[75.] Hai, C.H. and Chen, C.Y. (2001) Removal of metal ions and humic acid from water by iron-coated filter media. Chemosphere, 44, 1177–84.
[76.] Onyango, M.S., Kojima, Y., Matsuda, H. and Ochieng, A. (2003) Adsorption kinetics of arsenic removal from groundwater by iron-modified zeolite. Journal of Chemical Engineering of Japan, 36, 151G–22.
[77.] Wu, R.C., Qu, J.H. and Chen, Y.S. (2005) Magnetic powder MnO–Fe2O3 composite – a novel material for the removal of azo-dye from water. Water Research, 39, G30–8.
[78.] Wu, R.C., Qu, H.H., He, H. and Yu, Y.B. (2004) Removal of azo-dye Acid Red B (ARB) by adsorption and catalytic combustion using magnetic CuFe2O4 powder. Applied Catalysis B, 48, 49–5G.
[79.] Herrera, F., Lopez, A., Mascolo, G., Albers, E. and Kiwi, J. (2001) Catalytic combustion of Orange II on hematite: surface species responsible for the dye degradation. Applied Catalysis B, 29, 147–G2.
[80.] Takafuji, M., Ide, S., Ihara, H. and Xu, Z. (2004) Preparation of poly(1-vinylimidazole)-grafted magnetic nanoparticles and their application for removal of metal ions. Chemistry of Materials, 16, 1977–83.
[81.] Yavuz, C.T., Mayo, J.T., Yu, W.W., Parkash, A., Falkner, J.C., Yean, S.J., Cong, L.L., Shipey, H.J., Kan, A., Tomson, M., Nateson, D. and Colvin, V.L. (2006) Low-field magnetic separation of monodisperse Fe3O4 nanocrystals. Science, 314, 9G4–7.
[82.] Magnuson, M.L. and Speth, T.F. (2005) Quantitative structure-property relationships for enhancing predictions of synthetic organic chemical removal from drinking water by granular activated carbon. Environmental Science & Technology, 39, 770G–11.
[83.] Cornell, F.H. and Schwertmann, U. (199G) The Iron Oxide, 1st edn, John Wiley & Sons, Inc., New York.
[84.] Hsia, T.H., Lo, S.L., Lin, C.F. and Lee, D.Y. (1994) Characterization of arsenate adsorption on hydrous iron oxide using chemical and physical methods. Colloids and Surfaces A, 85, 1–7.
[85.] Munoz, J.A., Gonzalo, A. and Valiente, M. (2002) Arsenate adsorption by Fe(III)-loaded open-celled cellulose sponge: thermodynamic and selectively aspect. Environmental Science & Technology, 36, 3405–11.
[86.] Zhang, Y., Yang, M. and Huang, X. (2003) Arsenic(V) removal with a Ce(IV)-doped iron oxide adsorbent. Chemosphere, 51, 945–52.
[87.] Zhang, Y., Yang, M., Gao, Y.X., Wang, F. and Huang, X. (2003) Preparation and adsorption mechanism of rare earth-doped adsorbent for arsenic (V) removal from groundwater. Science in China Series B, 46, 252–8.
[88.] Zhang, Y., Yang, M., Dou, X.M., He, H. and Wang, D.S. (2005) Arsenate adsorption on a FeCe bimetal oxide adsorbent: role of surface properties. Environmental Science & Technology, 39, 724G–53.
[89.] Sun, D., Meng, T.T., Loong, T.H. and Hwa, T.J. (2004) Removal of natural organic matter from water using a nano-structured photocatalyst coupled with filtration membrane. Water Science and Technology, 49, 103–10.
[90.] Takafuji, M., Ide, S., Ihara, H. and Xu, Z. (2004) Preparation of poly(1-vinylimidazole)-grafted magnetic nanoparticles and their application for removal of metal ions. Chemistry of Materials, 16, 1977–83.
[91.] Wang, L., Yang, Z.M., Gao, J.H., Xu, K.M., Gu, H.W., Zhang, B., Zhang, X.X. and Xu, B. (2006) A biocompatible method of decorporation: bisphosphonate-modified magnetite nanoparticles to remove uranyl ions from blood. Journal of the American Chemical Society, 128, 13358–9.
[92.] Chen, W.J., Tsai, P.J. and Chen, Y.J. (2008) Functional Fe3O4/TiO2 core/shell magnetic nanoparticles as photokilling agents for pathogenic bacteria. Small, 4, 485–91.
[93.] Gong, P., Li, H.M., He, X.X., Wang, K.M., Hu, J.B., Tan, W.H., Zhang, S.C. and Yang, X.H. (2007) Preparation and antibacterial activity of Fe3O4@Ag nanoparticles. Nanotechnology, 18, 285G04.

[94.] El-Boubbou, K., Gruden, C. and Huang, X.F. (2007) Magnetic glyco-nanoparticles: a unique tool for rapid pathogen detection, decontamination, and strain differentiation. Journal of the American Chemical Society, 129, 13392–3.
[95.] Chang, S.C. and Adriaens, P. (2007) Nano-immunodetection and quantification of mycobacteria in metalworking fluids. Environmental Engineering Science, 24, 58–72.
[96.] Porter, J., Robinson, J., Pickup, R. and Edwards, C.J. (1998) An evaluation of lectin-mediated magnetic bead cell sorting for the targeted separation of enteric bacteria. Journal of Applied Microbiology, 84, 722–32.
[97.] Zhong, L.S., Hu, J.S., Liang, H.P., Cao, A.M., Song, W.G. and Wan, L.J. (2006) Self-assembled 3D flowerlike iron oxide nanostructures and their application in water treatment. Advanced Materials, 18, 242G–31.
[98.] Thackeray, M.M. (1997) Manganese oxides for lithium batteries. Progress in Solid State Chemistry, 25, 1–71.
[99.] Armstrong, A.R. and Bruce, P.G. (199G) Synthesis of layered LiMnO2 as an electrode for rechargeable lithium batteries. Nature, 381, 499–500.
[100.] Morales, A.M. and Lieber, C.M. (1998) A laser ablation method for the synthesis of crystalline semiconductor nanowires. Science, 279, 208–11.
[101.] Gowda, M.S., Kumar, P.S.K. and Kulkarni, R.M. (2014) Photo Catalytic Deprivation to Methylene Blue via ZnO Nano Particles by Advanced Oxidation Process. International Journal of Engineering Research, Vol. 2, Issue 4, ISSN: 2321-7758.
[102.] Gowda, M.S. and Kumar, P.S.K. (2014) Degradation of Methyl Orange Using Photo Catalyst (ZnO) and Doped Cu, Nano Particles By Advanced Oxidation Process. International Journal of Current Research, Vol. 6, Issue 08, pp. 8089-8094, ISSN: 0975-833X.